Journal of the Ceramic Society of Japan 112 [6] 321–326 (2004)

Paper

Sintering Curve Inflection in Densification of Fine CeO_2 Powders at High Temperature

Masakuni OZAWA

Ceramic Research Laboratory, Nagoya Institute of Technology, 10–6–29, Asahigaoka, Tajimi-shi, Gifu 507–0071

CeO_2 微粒子の緻密化における焼結曲線の屈曲

小澤正邦

名古屋工業大学セラミックス基盤工学研究センター，507–0071 岐阜県多治見市旭丘 10–6–29

The sintering behavior of fine cerium dioxide (CeO_2) powders from direct homogeneous precipitation using hexamethylenetetramine was examined by monitoring the continuous shrinkage of powder compacts during heating from 30 to 1700°C. Depending on the pre-heat-treatment condition of powders, the sintering curves of two starting powder compacts showed different shrinkage behavior. A powder heated at 650°C showed a normal sintering curve (S-type) with the highest shrinkage rate at around 1000°C. However, a powder heated at 350°C showed an extremely high shrinkage rate with inflection points in the sintering curve at 1300–1500°C. We analyzed the microstructure, pore structure and the secondary particle size of sintered bodies after sintering curve inflection. Grains 0.08 μm in size were roughly packed one another in the microstructure at 900°C after local sintering in the interior part of aggregated particles. The rapid shrinkage after rearrangement started at higher temperatures of 1300–1500°C, inducing large grain growth. The combination of rapid rearrangement and grain growth, which resulted in a sintering curve inflection, was assumed at temperatures as high as 900–1500°C.

[Received January 8, 2004; Accepted March 23, 2004]

Key-words : *CeO_2, Ceramics, Sintering, Powder, Dilatometry*

1. Introduction

Cerium dioxide (ceria, CeO_2) is a useful material for solid state electrochemical devices such as fuel cells, as well as automotive catalyst components.[1)–4)] Nanocrystalline powders of CeO_2 have been prepared by several different techniques to control sintering or heterogeneous catalysis.[5)–11)] In general, these particles have a tendency to agglomerate into larger secondary particles. The building units and nanocrystalline sizes vary during further heat treatment, so that the sintering behavior becomes complex. The mechanism for densification is still a subject needing clarification to improve sintering procedures or the thermal stability of heterogeneous catalysts. Because conventional processing such as uniaxial pressing and suspension coating result in complex situations involving compaction distribution and high friction forces in nanocrystalline powders,[12)–14)] various approaches to control the sintering of nanocrystalline powders must be studied for better processing of targeted devices. This study describes the sintering of nanocrystalline CeO_2 from nanocrystalline powders with agglomeration. The sintering behavior is examined using dilatometry and analyzed by microstructure and pore structure. The unique character of sintering, depending on the heat treatment condition applied to the same starting powder, was observed, and then a model for densification is presented. A combined process of rearrangement of particles and grain growth is evident in the sintering of a fine cerium oxide powder at temperatures up to 1700°C.

2. Experimental

The starting powder was synthesized by homogeneous precipitation.[5),10)] Aqueous solutions of 0.3 M hexamethylenetetramine (HMT) and 0.05 M cerium nitrate were prepared separately. Suitable amounts of these solutions were mixed with stirring in order to obtain a homogeneous solution, then held at 90°C for 24 h. The precipitate was separated from the solution by filtration, and washed with water, then dried at 120°C for 10 h in air. Different starting powders were obtained by heating the precipitate at 350°C or 650°C for 5 h in air.

The crystal phase and grain size of the powder were studied by X-ray diffraction (XRD) using a powder diffractometer (Rigaku rint200, Tokyo) with Cu Kα radiation. The average crystalline size was determined from peak broadening with reference to the diffraction pattern of coarse CeO_2 by Hall's method. The secondary particle size of aggregates was measured from photographs taken by scanning electron microscopy (SEM; JEOL, JMS6100, Tokyo). For comparison, small amounts of powder were investigated by transmission electron microscopy (TEM, JEOL 200CX, Tokyo). Nitrogen adsorption experiments at 77 K were carried out to determine the specific surface area by the Brunauer–Emmett–Teller (BET) method (Quantachrome, Autosorp 3b, Boyton Beach, FL, USA).

Powder compact bodies 5 mm long and 2×2 mm in cross section were prepared from two cerium oxide powders at room temperature by uniaxial pressing at 50 MPa. The apparent density of a starting sample was measured by the conventional procedure to measure the dimensions and weight of a compact body.

Sintering was monitored using a dilatometer (TD; Mac Science TD5200s, Kanagawa) in air at a heating rate of 5 K/min at temperatures up to 1700°C. The samples were quenched at selected temperatures without soaking. After degasing at 200°C, they were characterized by mercury porosimety (Fison Instruments, Pascal 240, Rodano–Milan, Italy) to measure pore distribution. SEM was used to observe the microstructure of the cerium oxide ceramic and to measure its grain size after heating and quenching at each temperature. The apparent density values of sintered ceramics were measured by water

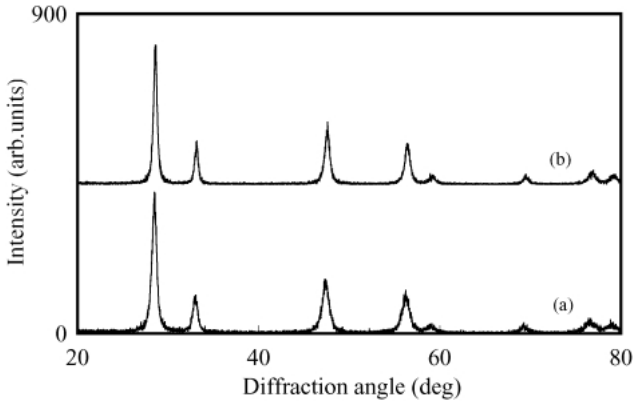

Fig. 1. X-ray diffraction pattern of cerium oxide from homogeneous precipitation with HMT, followed by heat treatment at (a) 350°C and (b) 650°C.

displacement.

3. Results

Figure 1 shows the X-ray diffraction pattern of the prepared powders. The peak widths are characteristic of low crystallinity as expected for low temperature calcination. The crystalline size calculated from the widths was 19 nm and 31 nm for the powders heated at 350°C and 650°C, respectively. A typical images of the powders obtained by a SEM and TEM are shown in **Figs. 2** and **3**, respectively. The particles show the agglomerated state of homogeneous particles with a size distribution around 0.05–0.2 μm in diameter, however the strength of these agglomerates seems to be weak. Therefore, they may behave as individual powders when pressed. The particle sizes determined by SEM were 0.08 μm and 0.10 μm for two powders heated at 350°C and 650°C, respectively. The primary crystalline sizes determined by TEM seemed to be 10–20 nm for a powder heated at 350°C and 10–50 nm for heated at 650°C, the average values of which corresponded to the crystalline size determined by XRD. The primary crystalline sizes (XRD), secondary particle sizes (SEM) and surface areas (BET) are listed in **Table 1**.

The linear shrinkage of a powder compact is shown in **Fig. 4**. The highest shrinkage occurs at 1000–1100°C in the powder heated at 650°C. However, in the case of the powder heated at 350°C, a highly accelerated shrinkage of the compact was observed at higher temperatures of 1300–1500°C, as determined by the derivative curve in **Fig. 5**. The contrasting results can be attributed to the starting powder structure with agglomerates, which may be formed in powders prepared by chemical techniques, followed by different low-temperature heat treatment. The behavior shown in Fig. 4(b) can be classified as a normal S-type sintering, showing higher shrinkage over a certain temperature range for a typical compacted powder. I have focused on the fast densification behavior for the other powder compact as shown in Fig. 4, which showed an inflection in its sintering curve and two peaks due to sintering rates at 1300–1500°C, as shown in Fig. 5. There is no structural transformation of CeO_2, unlike TiO_2,[15),16)] in these temperature ranges, thus the sintering inflection should be caused by a rapid change of the microstructure. In particulare, the apparent increase in density during the fastest densification step at 1500°C must be explained by an acceleration mechanism in addition to the normal sintering behavior.

The effect of the temperature during sintering on the grain

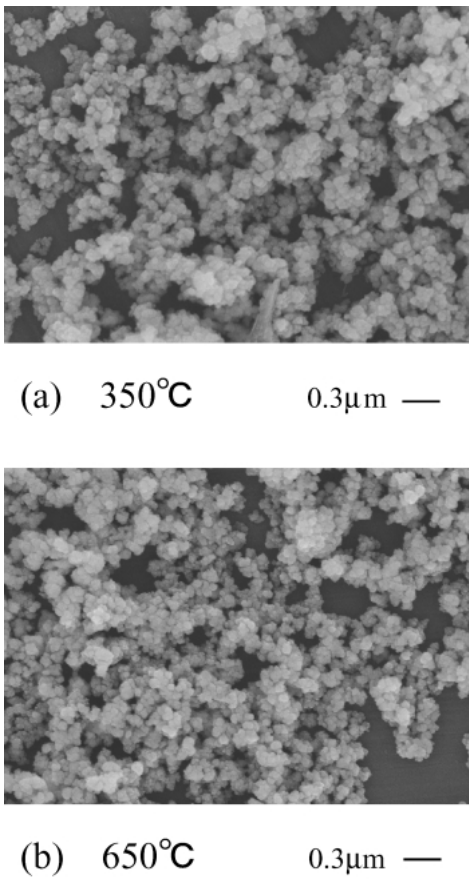

Fig. 2. SEM images of cerium oxide from homogeneous precipitation with HMT, followed by heat treatment at (a) 350°C and (b) 650°C.

sizes and pores in the sintered bodies is shown in the SEM images in **Fig. 6**. We measured the size distribution of each sintered and quenched body as shown in log-normal plots in **Fig. 7**. An increase in grain size was rarely observed at the temperatures up to 900°C; however, above 1100°C, a rapid increase was observed. The microstructure did not show a large change below 1100°C, as shown in Figs. 6(a)-(c). Above 1300°C, grain growth was obvious, as shown in Figs. 6 (d)-(f). The mean grain size increase at each temperature was measured at 0.08(0) μm for the sintered body at 700°C, 0.08 (2) μm at 900°C, 0.09(6) μm at 1100°C, 0.28 μm at 1300°C, 1.0 μm at 1500°C, and 11.0 μm at 1650°C. In addition, at 1300°C, the size distribution became bimodal, and the smaller grain size of 0.1 μm, the same as that at 1100°C, remained. A detailed examination of Fig. 6(d) revealed that its main microstructural feature is the nonuniform grain size with small pores, in which both partially connecting grains and isolated fine particles could be observed.

Figure 8 shows the pore distribution measured by porosimetry for sintered bodies at 900–1500°C without soaking. The measurement was carried out immediately before and after the fastest densification step, because the modifications of the pore size distribution depended mainly on the rapid grain growth. The total volume of pores was reflected by the relative density of bodies (Fig. 4). The cut off diameter in the pore volume curves was 0.06 μm at a sintering temperature of 900°C, 0.15 μm at 1300°C, and 0.35 μm at 1500°C, as shown in Fig. 8.

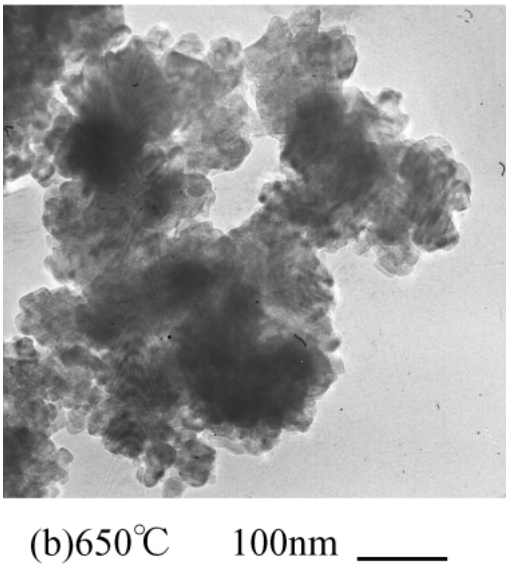

Fig. 3. TEM images of cerium oxide from homogeneous precipitation with HMT, followed by heat treatment at (a) 350°C and (b) 650°C.

4. Discussion

The results indicate the characteristics of very fast sintering rates for a powder heated at 350°C, particularly in the temperature range of 1300–1500°C, while such behavior is not observed for the other powder heated at 650°C, which shows

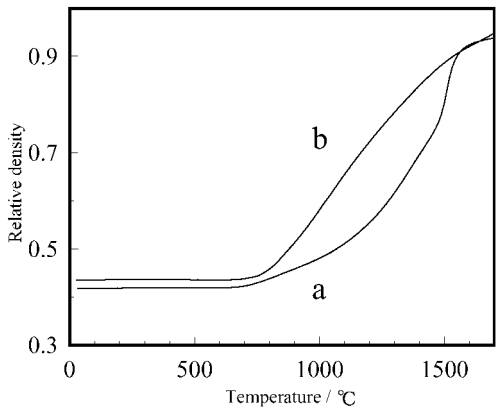

Fig. 4. Shrinkage of the compact using the powders after heat treatment at (a) 350°C and (b) 650°C as a function of temperature at a heating rate of 5 K/min.

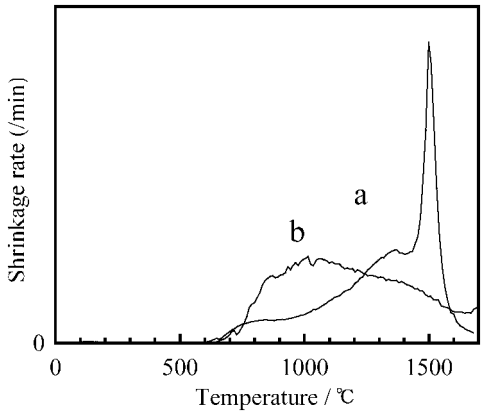

Fig. 5. Shrinkage rate of the powder compact as a function of temperature, calculated from the data in Fig. 3 for the powders heat-treated at (a) 350°C and (b) 650°C.

Table 1. Crystallite Size, Particle Size and Surface Area of Starting Powder Samples

Heating Tempearture (℃)	Phase*1	Crystalline size *2 (nm)	Aggregate size *2 (μm)	Surface area *3 (m^2/g)
350	Cubic CeO_2	19	0.08(0)	48.5
950	Cubic CeO_2	31	0.10(2)	36.0

*1 XRD, *2 XRD, *3 SEM, *4 N_2 adsorption at 77K (BET method)

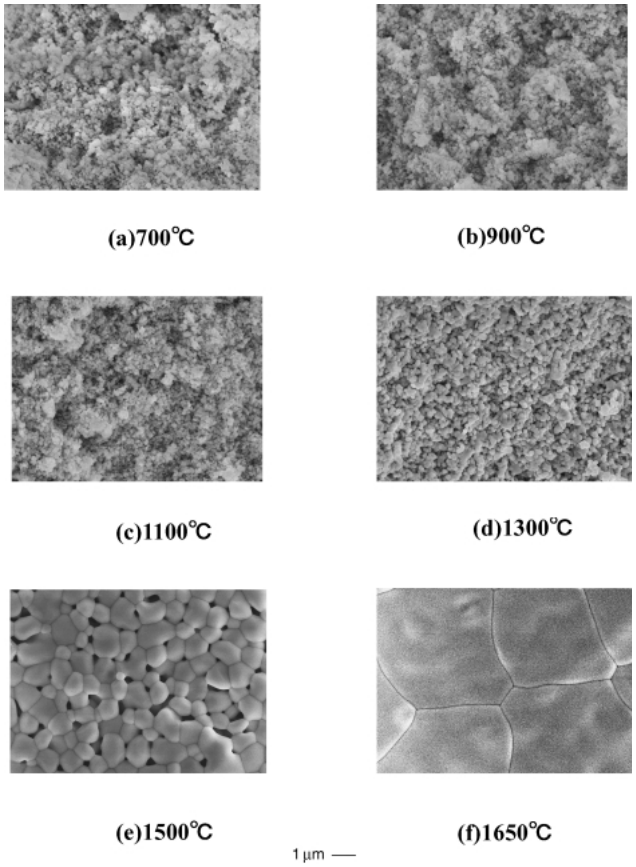

Fig. 6. SEM images of sintered ceramic powder heated at 350°C. The sintering temperature was (a) 700°C, (b) 900°C, (c) 1100°C, (d) 1300°C, (e) 1500°C and (f) 1650°C without soaking at a heating rate of 5 K/min.

normal sintering. A sample of close-packed, dense particles should exhibit a normal sintering curve. However, the agglomerates with fine crystalline size must experience sintering first in their interior before sintering between grains.

The variable feature between the two starting powders is the crystalline size, i.e. the primary particle size in the agglomerates. In general, the strength of agglomerates in powders often prepared by a chemical route is controlled by the extent of particle-particle interaction. Aside from several forces such as hydrogen bonding to surface hydroxyl groups, the size of units (the primary particle size) should be the important factor in forming bridges between adjacent particles. In this work, I assumed that each grain (when preheated at 350°C) after sintering below 900°C first became a dense powder, and then the sintering between grains started at higher temperatures. This initial stage was not clearly observed in the microstructure shown in the SEM images in Fig. 6, because of the low magnification. However, at the least, the information from SEM images indicates very small changes in the apparent microstructure or packing behavior of powder compacts without grain growth of the secondary particles, as shown in Figs. 6 (a)–(c). The sintering rate from dilatometry (as shown in Fig. 5) indicated the slow shrinkage of a compact at temperatures below 1100°C. Thus, below this temperature, sintering mainly occurs in the interior of the secondary particles, so that dense powders remain to be roughly packed. In subsequent steps at 900–1500°C, both the fast shrinkage rate and the microstructure seem to indicate that a grain rearrangement

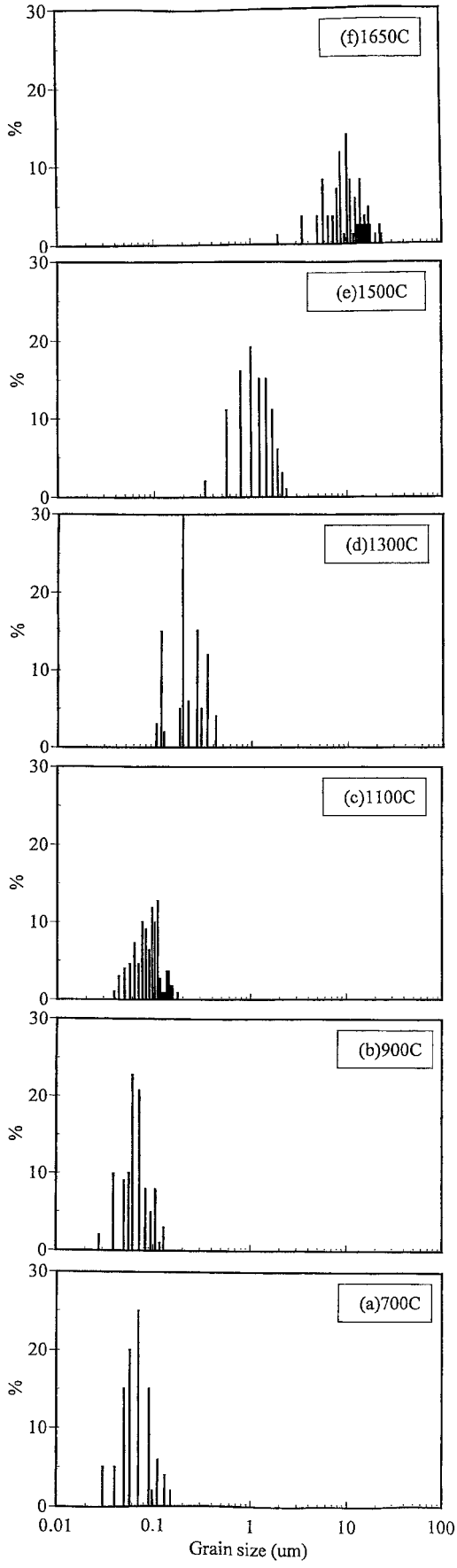

Fig. 7. Grain size distribution in CeO_2 sintered bodies from a powder heated at 350°C, followed by heating at temperatures of (a) 700°C, (b) 900°C, (c) 1100°C, (d) 1300°C, (e) 1500°C and (f) 1650°C without holding time at a heating rate of 5 K/min.

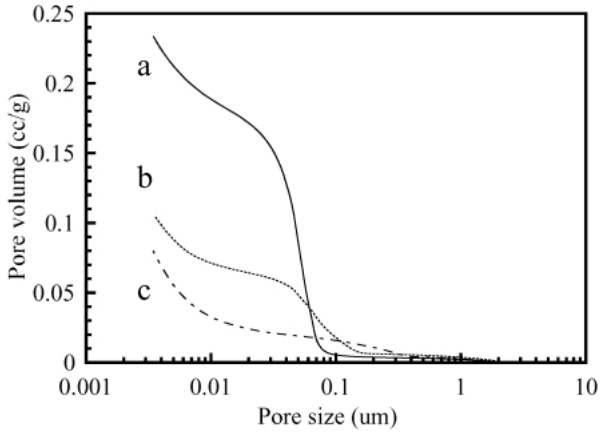

Fig. 8. Pore volume versus pore size for sintered bodies from a powder (heated at 350°C). Ceramics were sintered at temperatures of (a) 900°C, (b) 1300°C, and (c) 1500°C without holding time at a heating rate of 5 K/min.

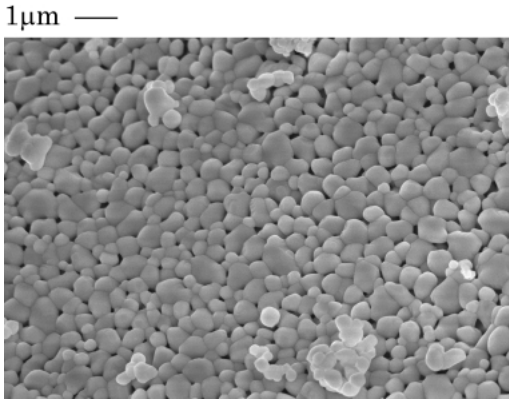

Fig. 9. SEM image of sintered ceramic powder heated at 650°C. The sintering temperature was 1300°C without soaking at a heating rate of 5 K/min.

process toward densification is coupled with grain growth. In general, the multiplication of local perturbations caused by rapid grain growth leads to a generalized grain rearrangement, and consequently, the microstructure evolves toward a more homogeneous microstructure. This feature can be seen in the SEM images in Figs. 6(d)–(e) for microstructures sintered at 1300–1500°C.

A detailed examination of Fig. 6(d) revealed that its main feature is the nonuniform grain size with small pores, in which the packing of both partially connecting grains and isolated fine particles could be observed. The grain size distribution measurement (Fig. 7(d)) also indicates the tendency to bimodal distribution with the maximum frequencies at 0.1 μm and 0.3 μm in diameter in the microstructure at 1300°C. The cut off diameters in the pore volume curves were 0.06 μm at the sintering temperature of 900°C, 0.15 μm at 1300°C, and finally, 0.35 μm at 1500°C, as shown in Fig. 8. The large distribution in pore sizes in the range of 0.05–0.15 μm is noted for a sintered body at 1300°C. This temperature corresponds to the first peak of the sintering rate as shown in Fig. 5(a). The rearrangement process can justify the amplitudes (the difference in sizes) in the bimodal size distribution (resulting in concurrent grain growth at 1500°C). The pore size distribution shown in Fig. 8(c) indicates the elimination of smaller pores 0.05–0.1 μm in size and a size increase to ca. 0.2 μm corresponding to the grain size increase.

The rearrangement of particles may be more possible in a more open particle network at a lower green density. Such rearrangement mechanisms should result in a coordinated repacking, an improved packing density and a homogenization of the microstructure. If this situation occurs in a high temperature range, the movement and grain growth are much faster than those in the lower temperature process. In this work, the sudden increase in the density, observed at 1300–1500°C (two peaks in Fig. 5(a)), could be explained by an improved packing density for the particles 0.3 μm in size, followed by a rapid grain growth. The arrangement at higher temperature could induce more rapid growth of particles due to a more highly thermally activated diffusion processes between grains newly in contact with one another. Thus, in the fine powder heated at 350°C, the combination of grain growth with rearrangement may be assumed to occur at 1300–1500°C. Chen and Chen[17),18)] proposed that particle coarsening leads to coordinated particle movement and an increase in packing density. They concluded that very fine, surface-active powders that coarsen rapidly are uniquely capable of taking advantage of coarsening-motivated homogenization and rearrangement densification processes at moderate temperatures. In the situation in this study, the combined process at high temperature, replacing a single rearrangement process, is assumed for rapid densification at 1300–1500°C. However, a simple particle coarsening mechanism cannot be excluded, because the accelerated densification rate in low density green bodies was observed at around 800°C. In addition, another repacking cycle might occur partially in a compact body even at around 1100°C. In this work, the repacking of powders inducing densification is complicated by continuing or repeated grain growth of the primary and secondary particles. This should be compared with the microstructure from a normal sintering process. **Figure 9** shows an SEM image of a sintered compact of a powder ((b), initially heated at 650°C) at 1300°C, demonstrating normal sintering with the uniform development of a grain boundary and grain growth before the full densification stage. The microstructure shown in Fig. 6(d) due to a repacking process features local sintering and the inhibition of grain growth and the possible fast sintering of fine powders at temperatures higher than 1300°C.

In conclusion, the sintering studies of nanosize CeO_2 powders with agglomeration have shown the influence of starting powder structure induced by pre-heat treatments. An accelerated inflection was clearly observed in the sintering curve by plotting relative density changes or shrinkage rates versus temperature. Rapid densification brought about particle rearrangement and grain growth during sintering. The occurrence of particle rearrangement at high temperatures was determined for a starting powder from a homogeneous precipitation. The fact that this mechanism is active even at temperatures as high as 1300–1500°C is an interesting phenomenon when very fine powders are used.

5. Summary

The sintering behavior of two cerium oxide powders from direct homogeneous precipitation using hexamethylenetetramine was examined by monitoring the continuous shrinkage of a powder compact during heating from 30 to 1700°C. Depending on the pre-heat treatment of the powders, sintering curves showed normal or abnormal behavior during shrinking. A powder heated at 650°C showed a normal S-type curve

on sintering with the highest shrinkage rate at around 1000°C. However, a powder heated at 350°C exhibited an extremely high shrinkage rate, showing inflection points in the sintering curve, at 1300°C and 1500°C. We analyzed the microstructure, pore structure and the secondary particle size of the sintered bodies. Below 900°C, each grain ca. 0.1 μm in size, the same as that of the starting powder, roughly packed in the microstructure. This arrangement at higher temperature should induce a more rapid growth of particles due to a more highly thermal-activated diffusion process between newly contacted grains. The combination of rapid rearrangement and grain growth was assumed at temperatures as high as 1300–1500°C.

References

1) Steele, B. C. H., *Solid State Ionics*, Vol. 129, pp. 95–110 (2000).
2) Eguchi, K., Setoguchi, T., Inoue, T. and Arai, H., *Solid State Ionics*, Vol. 52, pp. 165–172 (1992).
3) Sugiura, M., *Catalysis Surveys from Asia*, Vol. 7, pp. 77–85 (2003).
4) Ozawa, M., Kimura, M. and Isogai, A., *J. Alloy Compds.*, Vol. 193, pp. 73–75 (1993).
5) Hsu, E., Ronnquist, L. and Matijevic, E., *Langumuir.*, Vol. 4, pp. 31–37 (1988).
6) Chen, P.-L. and Chen, I.-W., *J. Am. Ceram. Soc.*, Vol. 76, pp. 1577–1583 (1993).
7) Zhou, V., Phillips, R. J. and Switzer, J. A., *J. Am. Ceram. Soc.*, Vol. 78, pp. 981–985 (1995).
8) Djuricic, B. and Pickering, S., *J. Eur. Ceram. Soc.*, Vol. 19, pp. 1925–1934 (1999).
9) Ozawa, M., *Script. Mater.*, Vol. 50, pp. 61–64 (2004).
10) Ozawa, M., Hibi, H. and Suzuki, S., *Huntai oyobi Hunmatu Yakin* (*J. Jpn. Soc. Powder Powder Metall.*), Vol. 50, pp. 354–358 (2003).
11) Suda, E., Pacaud, B., Montardi, Y., Mori, M., Ozawa, M. and Takeda, Y., *Electrochemistry*, Vol. 71, pp. 866–872 (2003).
12) Lange, F. F., *J. Am. Ceram. Soc.*, Vol. 72, pp. 3–12 (1989).
13) Kumar, K. N., Keiser, K., Burggraaf, A. J., Okubo, T., Nagamoto, H. and Morooka, S., *Nature*, Vol. 358, pp. 48–51 (1992).
14) Allen, A., Krueger, S., Skandan, G., Long, G. G., Hahn, H., Kerch, H. M., Parker, J. and Ali, M. N., *J. Am. Ceram. Soc.*, Vol. 79, pp. 1201–1215 (1996).
15) Echeverria, L., "Ceramic Transactions," Vol. 12, Ed. by. Messing, G. L., Hirano, S. and Hausner, H., Am. Ceram. Soc., Westerville, OH (1990) pp. 649–658.
16) Kim, D. W., Kim, T. G. and Hong, K. S., *J. Am. Ceram. Soc.*, Vol. 81, pp. 1692–1694 (1998).
17) Chen, P. L. and Chen, I. W., *J. Am. Ceram. Soc.*, Vol. 79, pp. 3129–3141 (1996).
18) Chen, P. L. and Chen, I. W., *J. Am. Ceram. Soc.*, Vol. 80, pp. 637–645 (1997).